Possible solar wind effect on the northern annular mode and northern hemispheric circulation during winter and spring

Hua Lu,[1] Martin J. Jarvis,[1] and Robert E. Hibbins[1]

[1]   Statistically measurable responses of atmospheric circulation to solar wind dynamic pressure are found in the Northern Hemisphere (NH) zonal-mean zonal wind and temperature, and on the Northern Annular Mode (NAM) in winter and spring. When December to January solar wind dynamic pressure ($P_{sw\mathrm{DJ}}$) is high, the circulation response is marked by a stronger polar vortex and weaker sub-tropical jet in the upper to middle stratosphere. As the winter progresses, the Arctic becomes colder and the jet anomalies shift poleward and downward. In spring, the polar stratosphere becomes anomalously warmer. At solar maxima, significant positive correlations are found between $P_{sw\mathrm{DJ}}$ and the middle to late winter NAM all the way from the surface to 20 hPa, implying a strengthened polar vortex, reduced Brewer–Dobson circulation and enhanced stratosphere-troposphere coupling. The combined effect of high solar UV irradiance and high solar wind dynamic pressure in the NH middle to late winter is enhanced westerlies in the extratropics and weaker westerlies in the subtropics, indicating that more planetary waves are refracted toward the equator. At solar minima, there is no correlation in the NH winter but negative correlations between $P_{sw\mathrm{DJ}}$ and the NAM are found only in the stratosphere during spring. These results suggest possible multiple solar inputs that may cause refraction/redistribution of upward wave propagation and result in projecting the solar wind signals onto the NAM. The route by which the effects of solar wind forcing might propagate to the lower atmosphere is yet to be understood.

Citation: Lu, H., M. J. Jarvis, and R. E. Hibbins (2008), Possible solar wind effect on the northern annular mode and northern hemispheric circulation during winter and spring, *J. Geophys. Res.*, *113*, D23104, doi:10.1029/2008JD010848.

1.   Introduction

[2]   The Northern Annular Mode (NAM) is a planetary-scale pattern of atmospheric variability that is marked by a deep and out of phase relationship in the zonal wind anomalies along ~55°N and ~35°N [*Baldwin*, 2001; *Thompson et al.*, 2003]. The NAM is a meridional oscillatory pattern between the subtropics and the polar region and is characterized by zonally symmetric meridional meanderings of the extratropical jet [*Thompson and Wallace*, 1998]. In general, a stronger and colder polar vortex is found when the NAM is in its positive phase, while a weaker and warmer polar vortex is found when the NAM is in its negative phase [*Baldwin and Dunkerton*, 2001]. The NAM fluctuates the most during the northern hemispheric (NH) winter, when evidence shows that long-lived anomalies in the stratospheric NAM frequently precede similarly persistent anomalies in the tropospheric NAM, implying a stratospheric influence on the troposphere [*Thompson and Wallace*, 1998; *Baldwin*, 2001]. On time scales greater than one month, the NAM is highly correlated with the North Atlantic Oscillation (NAO) [*van Loon and Rogers*, 1978; *Hurrell*, 1995], and the Arctic Oscillation (AO) [*Thompson and Wallace*, 1998].

[3]   The total solar irradiance varies by about 0.1%, while the solar radiation in the ultraviolet (UV) part of the spectrum varies by about 5–8% over an 11-yr solar cycle (11-yr SC) [*Lean et al.*, 1997]. The UV radiative forcing is strongest near the stratopause, where the solar UV is most effectively absorbed by ozone [*Haigh*, 2003; *Hood*, 2004]. As a result of *in situ* photolysis in the upper stratosphere, higher solar UV inputs at solar maxima cause thermal perturbations by increasing the temperature gradient between the tropics and the winter pole [*Haigh*, 1994, 1996]. In turn, it alters the upward propagation of planetary-scale waves as well as the Brewer–Dobson (BD) circulation, resulting in a strengthened polar vortex and dynamic feedback in the lower atmosphere [*Kodera and Kuroda*, 2002]. Numerous studies have revealed compelling evidence for the signature of the 11-yr SC in atmospheric wind and temperature [*Labitzke and van Loon*, 1988; *Shindell et al.*, 1999; *Matthes et al.*, 2004; *Crooks and Gray*, 2005; *Labitzke et al.*, 2006; *Salby and Callaghan*, 2006; *Camp and Tung*, 2007]. Nevertheless, questions remain as to why general circulation models (GCMs) often predict a much smaller atmospheric response to the 11-yr SC than the observed solar signals, and how the rather weak solar forcing is amplified into larger than expected signals in meteorological parameters [*Hoyt and Schatten*, 1997;

---

[1]Physical Sciences Division, British Antarctic Survey, Cambridge, UK.

Austin et al., 2007]. The discrepancy between modeled and observed solar signals suggests either that the solar influence on climate might be greater than anticipated from solar UV radiative forcing alone, or that there are some processes inadequately represented by the GCMs.

[4] Possible solar influences on the NAM have been reported in the literature. *Ruzmaikin and Feynman* [2002] found that the NAM was skewed more negatively all the way vertically through the stratosphere and troposphere during the winters when solar activity is low (LS), while no clear tendency in the NAM was detected when solar activity is high (HS). *Kodera* [2002, 2003] found that the spatial pattern of the winter NAO is confined to the Atlantic sector at LS, whereas it shows a hemispherical structure at HS. *Ogi et al.* [2003] showed that the spring/summer circulation correlates well with the previous winter NAO at HS, whereas no significant correlation was found at LS. *Gimeno et al.* [2003] found that the NAO is positively correlated to the Northern Hemisphere (NH) surface temperature during HS winters, while no significant correlation was found during LS winters. These observational studies seem to suggest that the 11-yr SC modulates the NAM in a systematic manner. Such a modulation is intriguing as no direct causal mechanism connecting the 11-yr SC and the NAM has been obtained.

[5] Correlations have been found between solar wind driven geomagnetic activity and atmospheric variables including temperature, geopotential height and the NAO [*Boberg and Lundstedt*, 2002, 2003; *Thejll et al.*, 2003; *Palamara and Bryant*, 2004; *Bochnicek and Hejda*, 2005]. For the period of 1973 to 2000, *Boberg and Lundstedt* [2002, 2003] showed that the variation of the winter NAO was positively correlated with the electric field strength of the solar wind, and suggested a solar wind generated electromagnetic disturbance in the ionosphere might dynamically propagate downward to affect the NAO. For the period from the mid-1970s to the late 1990s, *Bochnicek and Hejda* [2005] found that the winter NAO was more positive when the geomagnetic index Ap is high, in line with the results of *Boberg and Lundstedt* [2002, 2003]. It is however apparent that a multi-decadal scale modulation of the relationship between the NAO and geomagnetic activity may exist, as the correlation tends to wax and wane over time-scales of a few decades [*Bucha and Bucha*, 1998; *Thejll et al.*, 2003; *Palamara and Bryant*, 2004]. *Lu et al.* [2007] demonstrated that there were multiple solar influences on atmospheric temperature, with both solar irradiance and solar wind drivers playing a role. They used the Ap index [*Mayaud*, 1980] as a measure of geomagnetic activity, which is indirectly dependent upon the solar wind characteristics. They showed that, for the period 1958–2004, the magnitude of the temperature response in the troposphere and the lower stratosphere to the geomagnetic Ap index is at least comparable to that associated with solar irradiance over the 11-yr SC.

[6] The transfer of energy from the solar wind to the Earth system is a complex process and can depend upon various solar wind parameters [*Wang et al.*, 2006]. *Palmroth et al.* [2004] have presented direct evidence for the dependence of Joule heating, generated by currents in Earth's upper atmosphere, on solar wind dynamic pressure. These currents are driven in the outer magnetosphere by solar wind action and connect to make a circuit through the auroral zones in the lower thermosphere region where they dissipate energy. They can be divided into "region 1" currents that flow down into the dawnside and up from the duskside of the higher latitude auroral zone and "region 2" shielding currents, with the opposite sense to "region 1" currents, which flow into and out of the lower latitude auroral zone. *Palmroth et al.* [2004] pointed out that both the "region 2" currents and the weaker "region 1" currents are highly correlated with magnetospheric pressure changes which are, in turn, balanced with changes in the solar wind dynamic pressure. They showed (their Figure 4) through magnetohydrodynamic numerical simulation that the Joule heating from these current systems is approximately proportional to the solar wind dynamic pressure. Hence, if solar wind geo-effectiveness is determined by the subsequent dissipation of magnetospheric energy into the neutral atmosphere through Joule heating, then the solar wind dynamic pressure can be used as a proxy for this geo-effectiveness.

[7] The importance of the solar wind dynamic pressure in transferring energy from the solar wind to the Earth's atmosphere has been demonstrated by several authors. *Shue and Kamide* [2001] showed that, in a magnetic cloud, increasing solar wind density intensified the auroral electrojets for both southward and northward interplanetary magnetic field (IMF). *Boudouridis et al.* [2003] demonstrated that, under IMF southward conditions, enhanced solar wind dynamic pressure widened the auroral oval and decreased the polar cap size. *Lu et al.* [2004] reported that compressional waves from within the solar wind dynamic pressure enhancements could lead to penetration of solar wind matter and energy across the magnetopause into the magnetosphere. *Palmroth et al.* [2007] analyzed 236 solar wind pressure pulses which were separated into two groups, dependent upon whether the solar wind magnetic field increased or decreased at the time of the pressure pulse. They showed that both groups transfer energy to the magnetosphere; although coupling efficiency decreased when the magnetic field increased, and vice versa, the coupling energy within the pressure pulses with increased magnetic field remained the larger. *Zhou and Tsurutani* [1999] have shown that sudden increases in the solar wind dynamic pressure can generate global disturbances with auroral activity appearing on the dayside and propagating to the nightside with ionospheric speeds consistent with the solar wind pressure pulse speed. In support of this, the inverse effect has been observed by *Liou et al.* [2006] whereby decreasing pressure pulses lead to a rapid extinguishing of auroral activity. Observations by *Laundal and Østgaard* [2008] indicate that the causative mechanism behind proton aurora precipitation during high dynamic pressure is connected to the compression of the magnetosphere, which is directly related to the solar wind dynamic pressure.

[8] Most of the above studies address transient events, *Zhou and Tsurutani* [2003] have shown that auroral intensity also responds to gradual changes in the solar wind dynamic pressure. They suggested that the production mechanism for persistent aurora during high solar wind pressure may differ from those for transient events and could be related to Kelvin–Helmholtz waves on the magnetospause. Similarly, *Liou et al.* [2007] showed that the more the magnetosphere was compressed, the more intense the global aurora. They
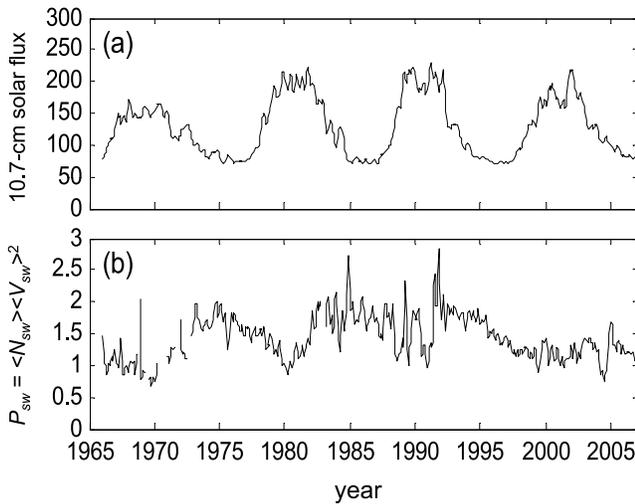
Figure 1. Time series of monthly mean (a) 10.7-cm solar flux in solar flux units (1 sfu = 10^{-22} Wm^{-2} Hz^{-1}) and (b) solar wind dynamic pressure P_{sw} in units of 10^{18} n m^{-1} s^{-2}.

suggested that the increase could be due to the fact that, taking a fixed L-shell, the equatorial magnetic field change under compression would be larger than that for the low altitude field-line mirror-points; the consequent increase in loss cone would increase particle precipitation.

[9] To date, no study has been carried out to examine possible perturbations of energy inputs by the solar wind on the NAM and, consequently, on the extratropical circulation. With better and longer solar wind and atmospheric data now available, it has become feasible to undertake such an investigation. In addition, it is necessary to examine how the 11-yr SC modulates the signals of the solar wind forcing during winter, when the thermal perturbation by the 11-yr SC is the largest, and a greater variation of the NAM prevails.

[10] Here, a statistical assessment of solar wind dynamic pressure forcing on the NAM and its vertical structure is carried out for the NH winter and spring months, when troposphere/stratosphere coupling is most vigorous and the zonal flow in the lower stratosphere is often disturbed by upward propagating waves from the troposphere [*Thompson and Wallace*, 2000]. We aim to address three research questions: (1) does the NAM respond to solar wind forcing during the NH winter? (2) if a response is identified, can we interpret the dynamic consequence of such a signature? (3) how do the NAM and atmospheric circulation respond to solar wind forcing given the different circulation conditions during high and low solar activity - namely, how does the 11-yr SC modulate the signature of solar wind forcing in the NAM and extratropical circulation?

2. Data and Methods

[11] Here the solar wind dynamic pressure, defined as $P_{sw} = N_{sw} V_{sw}^2$, where V_{sw} is the flow speed (m s^{-1}) and N_{sw} is the proton density (n m^{-3}, where n stands for particle number), is used as a proxy for solar wind energy transfer to the Earth's atmosphere. In this study, we use monthly averages to search for persistent and accumulative perturbations of P_{sw} on the stratospheric and tropospheric wind and temperature fields. In this study, the longer-time

response due to changes in monthly averaged P_{sw} is considered. Because the NAM and lower atmospheric variables have large internal variability on timescales less than one month, using monthly averages allows us to restrict the large random effects of internal variability.

[12] Homogeneous observations of solar wind measurements over a few solar cycles are necessary when investigating the Sun's long-term effect on the Earth's climate. Daily averages of V_{sw} and N_{sw} were used, obtained from the OMNI 2 data set in Geocentric Earth Magnetic (GEM) coordinates, supplied by the National Space Science Data Centre of NASA (http://gsfc.nasa.gov). This data set is produced from solar wind data collected by 15 geocentric satellites and 3 spacecraft in orbit around the L1 Sun-Earth Lagrange point and has been carefully compiled through cross-calibration. Though daily averages of V_{sw} and N_{sw} are available from 1963 onward, the temporal coverage before August 1965, and also between September 1982 and October 1994, is below 50% at hourly resolution, with ~8−15 complete days showing as missing data in each month [*King and Papitashvili*, 2005; *Finch and Lockwood*, 2007]. Thus monthly averages for those periods are not as reliable as for other periods. In this study, monthly averages of solar wind P_{sw} from 1966 to 2006, covering nearly 4 solar cycles, are used. P_{sw} is estimated as $\langle N_{sw} \rangle \langle V_{sw} \rangle^2$, where $\langle\ \rangle$ denotes monthly averages for the given variable. Our statistical analysis suggests that, although qualitatively similar results can be obtained by using $\langle N_{sw} V_{sw}^2 \rangle$, statistically more significant results are obtained when $\langle N_{sw} \rangle \langle V_{sw} \rangle^2$ was used. This likely to be because the correlation results from $\langle N_{sw} V_{sw}^2 \rangle$ are more affected by high frequency variations and missing values of the daily data.

[13] As solar irradiance was not directly measured for the entire period from 1966 to 2006, monthly averages of 10.7 cm solar radio flux (F_s, 1 sfu = 10^{-22} Wm^{-2}Hz^{-1}) were downloaded from the National Geophysical Data Center (NGDC) website (www.ngdc.noaa.gov/stp/). Figures 1a and 1b show the time series of monthly mean F_s and P_{sw} from 1966 to 2006. The correlation coefficient between F_s and P_{sw} is −0.26. Before the mid-1980s, P_{sw} tended to peak at LS but there is no clear correspondence between F_s and P_{sw} afterward.

[14] December to January mean solar wind dynamic pressure P_{swDJ} was used as a measure of solar wind forcing in the NH winter. Winters with values of P_{swDJ} greater or smaller than its average $\overline{P_{swDJ}}$ (= 1.5×10^{18} n m^{-1} s^{-2}) are classified as high P_{sw} (HP) and low P_{sw} (LP) winters, respectively. Note that similar results are obtained if the median value of P_{swDJ} is used for grouping HP and LP winters. It has been shown that solar UV influence on stratospheric ozone, and consequently stratospheric dynamics, takes place primarily in early winter [*Kodera*, 2002; *Matthes et al.*, 2004; *Kodera and Kuroda*, 2005; *Matthes et al.*, 2006]. For this reason, November to December mean 10.7 cm solar flux ($F_{s \text{ ND}}$) was used as an index to define solar irradiance forcing in early winter. Note that similar results are obtained if November to January mean F_s is used. In this study, winters with values of $F_{s \text{ ND}}$ greater or smaller than the average solar flux $\overline{F_{s_{ND}}}$ (=129 sfu) are grouped into high solar activity (HS) and low solar activity (LS) winters. For all our analyses, either the NAM or the atmospheric dynamic variables are stratified

according to HP and LP in relation to solar wind forcing, or HS and LS in relation to solar irradiance forcing.

[15] Our analyses are based on monthly mean zonal wind and temperature from the European Centre for Medium-Range Weather Forecasting (ECMWF) 40-yr reanalysis (ERA-40) (September 1957 to August 2002, [*Simmons and Gibson*, 2000]) and the ECMWF Operational analyses (September 2002 to December 2006, http://www.ecmwf.int/products/data/archive/descriptions/od/oper). Both data sets are available on the same 1.125° grid. ERA-40 has 23 vertical levels ranging from 1000 to 1 hPa while the Operational data have 21 levels at the same pressure levels as ERA-40 except for 600 and 775 hPa. We linearly interpolated the Operational data to these missing levels after the data are zonally averaged. To avoid contamination by the temporary heating caused by volcanic aerosols in the stratosphere, two year of data following two major eruptions (i.e., El Chichón in March 1982, and Pinatubo in June 1991) were excluded from our composite analyses. Zonal-mean zonal wind and temperature were deseasonalized by removing the long-term mean seasonal cycle from the data for the entire period of 1966–2006. For the composite analyses, the seasonal cycle was estimated by excluded those years affected by volcanic eruptions. We find that qualitatively similar results are obtained if the volcanic affected years are included.

[16] The NAM is defined as the leading empirical orthogonal function (EOF) of monthly mean geopotential height anomalies over 20°–90°N [*Baldwin and Dunkerton*, 1999, 2001]. We use monthly mean NAM derived from its daily values estimated from both the National Centers for Environmental Prediction (NCEP) reanalysis and blended ERA-40 and ECMWF Operational analyses for the same period of 1966–2006. The NAM derived from NCAR/NCEP reanalysis has 17 vertical levels ranging from 1000 to 10 hPa, while the NAM derived from ERA-40 has 23 vertical levels ranging from 1000 to 1 hPa. For simplicity, the NAM derived from NCEP reanalysis is referred to here as NCEP-NAM and that derived from ERA-40 and Operational data is referred to as ERA40-NAM. The winter is designated by the year in which January falls.

[17] The main diagnostic tools employed are composite analysis and linear correlation. Serial correlation in the wind and temperature data could cause spurious inflation of statistical confidence. To correct this, we calculated the effective number of degrees of freedom n in the same manner as *Davis* [1976], which was derived in the context of autoregressive models for moderate number of data samples. The statistical significance of the correlation was then estimated using a Student's t-test against the null hypothesis of zero correlation with $n \sim 2$ degrees of freedom. That is: the p-value was calculated as $r(n-2)^{\frac{1}{2}}(1-r^2)^{-\frac{1}{2}}$, where r is the correlation coefficient, and the confidence level (%) is quoted as $(1 \sim p) \times 100$. The same Monte Carlo significance test used by *Lu et al.* [2007] was used to test the statistical significance of the composite differences.

3. Results

3.1. Composite Analysis Stratified According to Solar Wind Dynamic Pressure

[18] Figure 2 shows the composites of deseasonalized zonal-mean zonal wind (line contours) and temperature (color contours) during HP (left panels), and during LP (right panels) for December to April (from top to bottom). It shows that, under HP, the seasonal progression of deseasonalized extratropical zonal wind is clearly marked by a poleward and downward movement (Figures 2c, 2e, 2g, and 2i). Westerly anomalies first appear in the mid-latitude upper stratosphere in December (Figure 2a). A dipole structure that comprises easterly anomalies near the subtropical upper stratosphere and westerly anomalies in the Arctic stratosphere emerges in January (Figure 2c). This dipole structure intensifies and extends to the middle to lower stratosphere in February (Figure 2e). In March, the westerly anomalies have descended into the low stratosphere and the troposphere and the easterly anomalies have moved poleward (Figure 2g). In April, the easterly anomalies descend to the middle and lower stratosphere while the westerly anomalies become substantially weakened (Figure 2i). The corresponding temperature change in the extratropical stratosphere is cooling in December through February and warming in March and April while the opposite holds in the Arctic troposphere. Overall, the left panel of Figure 2 suggests a stronger and colder polar vortex and a weaker subtropical jet in the NH winter when solar wind forcing is enhanced. The magnitude of wind differences between polar westerly anomalies and subtropical easterly anomalies is up to 9 m s^{-1} in February. The magnitude of temperature anomalies in the polar region is up to $\sim$3 K in the winter and 4 K in spring.

[19] The right-hand panels of Figure 2 show that, in the extratropical stratosphere, nearly opposite wind and temperature anomalies appear under LP. In December, easterly anomalies appear in the subtropical to mid-latitude upper stratosphere, suggesting a weakened stratopause jet (see Figure 2b). In January, the easterly anomalies have moved to the polar region while westerly anomalies emerge in the subtropical to mid-latitude upper stratosphere. From January through March, a downward movement of these easterly anomalies is clearly visible (Figures 2d, 2f, and 2h). The downward descent of these easterly anomalies in the polar region is accompanied by the development of westerly anomalies in the subtropical and mid-latitude stratosphere in January and February and above in the Arctic upper stratosphere in March. In April, westerly anomalies appear in the Arctic stratosphere and easterly anomalies emerge in the subtropical stratosphere. In the Arctic, the corresponding temperature shows a steady downward extension of heating anomalies from December through March. In March, the polar temperature anomalies are characterized by a dipole pattern with a cooling cell above 50 hPa and warming cell below (Figure 2h). In April, the Arctic stratosphere becomes anomalously colder while the extratropical stratospheric winds become anomalously more westerly (Figure 2j). Overall, the right-hand panels of Figure 2 suggest a weaker and warmer polar vortex in winter and stronger and colder polar winds in spring when solar wind forcing is low. The magnitude of wind differences between polar easterly anomalies and subtropical westerly anomalies is up to 8 m s^{-1} while the magnitude of warming and cooling in the polar stratosphere is up to $\pm$3–4 K.

[20] Figure 3 shows the composite differences between HP and LP (i.e. HP $\sim$ LP) for zonal wind (left panels) and temperature (right panels). Overall, the seasonal progres-
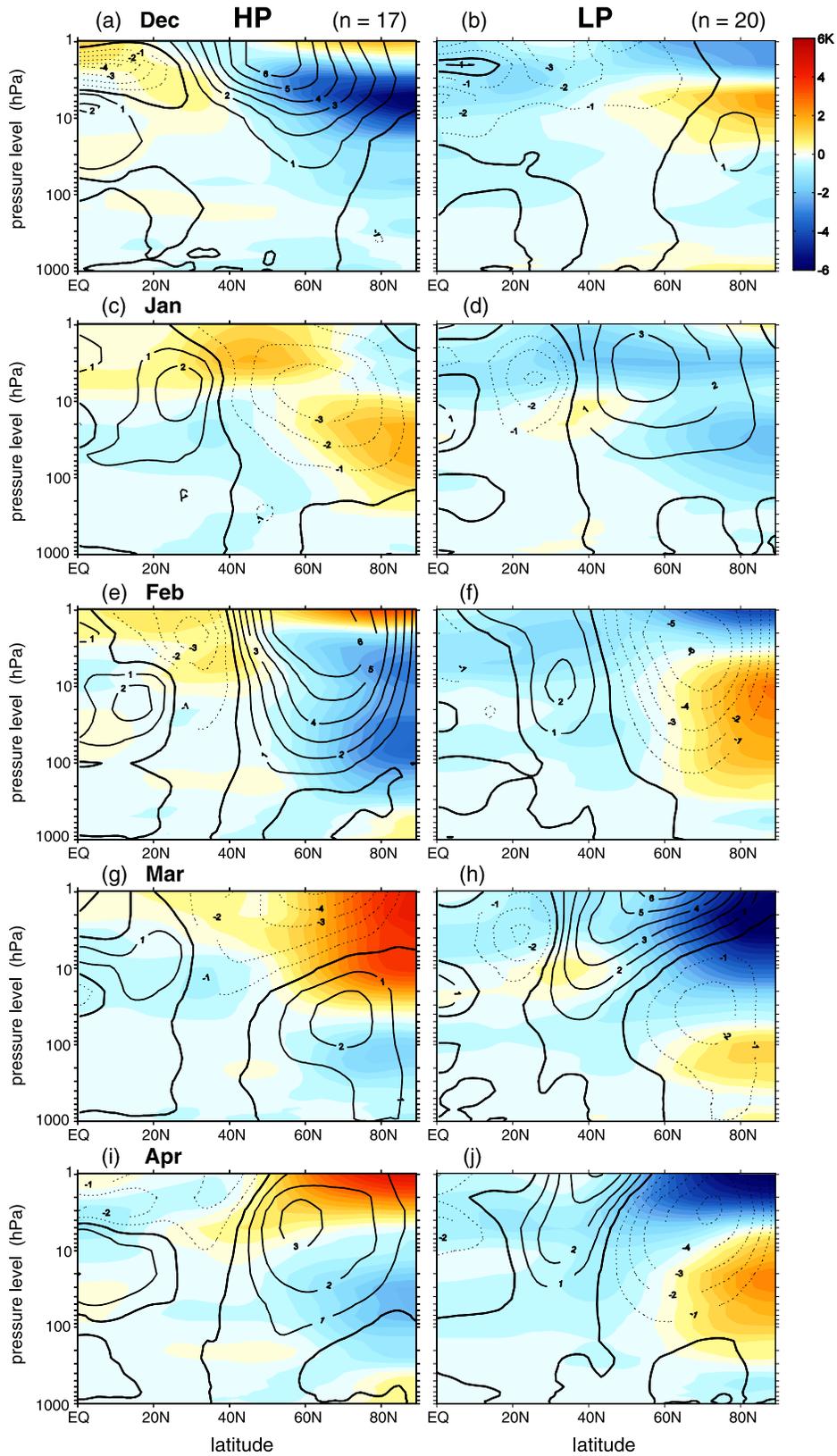
Figure 2

sions of the wind and temperature differences resemble those composite under HP, but with nearly doubled magnitude. It shows that the extratropical wind and temperature differences are significant at confidence levels above 90%, and the significance becomes more noticeable in late winter.

3.2. Influences on the NAM and the NH Circulation

[21] It has been shown that the NAM is manifested by vertically coherent variations in the extratropical winds, which are characterized by deep, zonally symmetric fluctuations in atmospheric pressure between the polar region and the mid-latitudes [*Thompson and Wallace*, 1998]. The well-organized circulation differences under HP and LP are likely to cause changes to the refraction of planetary wave propagation and hence to the meridional circulation at lower levels [*Haynes et al.*, 1991]. The observed changes of mean wind and temperature in the upper stratosphere in December may be amplified by the eddy-mean-flow feedback [*Kodera and Kuroda*, 2002, 2005]. It is known that changes in momentum deposition by large-scale planetary wave breaking are typically projected onto the NAM [*Kushner and Polvani*, 2004; *Gerber and Vallis*, 2007]. The main aim of this section is to examine possible influences of P_{swDJ} on the NAM and possible modulation effect of the 11-yr SC.

[22] Figure 4 shows the time series of January–February mean ERA40-NAM near the tropopause at 150 hPa (Figure 4a), December–January mean solar wind dynamic pressure P_{swDJ} (Figure 4b), and November–December mean 10.7-cm solar flux $F_{s\,ND}$ (Figure 4c). It shows that the NAM$_{JF}$ at 150 hPa is not correlated well with either P_{swDJ} ($r = 0.37$) or $F_{s\,ND}$ ($r = 0.20$). As it is evident in Figure 1, P_{swDJ} and $F_{s\,ND}$ are weakly correlated, with a negative correlation coefficient of −0.49, as faster solar wind speed tends to occur at solar minima.

[23] Figure 5 shows that significant correlation between the NAM$_{JF}$ at 150 hPa and P_{swDJ} exists only when $F_{s\,ND}$ is high. At HS, the NAM$_{JF}$ derived from either the NCEP reanalysis or blended ERA-40 and Operational data sets correlates positively with P_{swDJ}, with $r = 0.74$ and 0.8 respectively. Such correlations are highly significant at >99% confidence levels. At LS however no significant correlation is obtained ($r < 0.2$). In general, the NAM$_{JF}$ is smaller and more negative at LS than at HS. We found that this feature holds for other pressure levels from 1000 hPa to 20 hPa (not shown), consistent with *Ruzmaikin and Feynman* [2002]. The red shaded data samples in Figure 5 indicate years when a major Stratospheric Sudden Warming (SSW) occurred. Their distribution suggests that, at HS and in January and February, major SSWs are more likely to occur when P_{swDJ} is low. At LS however the occurrence of major SSWs is independent of P_{swDJ}, and more likely to occur when NAM$_{JF}$ is low. The correlation patterns remain

similar when either the NAM$_{JF}$ derived from NCEP or that derived from blended ERA-40 and Operational data is used.

[24] Figure 6 shows the correlations between P_{swDJ} and the January, February, and March NAM (1st, 2nd, and 3rd columns), and January through March mean NAM (4th column) when F_{sDJ} is high; results are shown where NCEP-NAM (upper panels) and the ERA40-NAM are used (lower panels). It shows that for individual months and the January–March average, similar vertical correlation patterns hold for either the NCEP-NAM or the ERA40-NAM at all the pressure levels below 10 hPa. From the surface to 20 hPa, the January and February NAMs are highly correlated to P_{swDJ}, while weaker correlations are found in March. The highest correlations are found in February with maximum correlation coefficient $r_{max} = 0.8$ at 200 hPa, and $r > 0.5$ all the way from 1000 hPa to 50 hPa. In January and March, the vertical pattern of the correlations shows a double-peak altitude profile with one peak near the surface and another near 100–200 hPa, with a minimum at 300–400 hPa. The correlation coefficients between P_{swDJ} and NAM$_{JFM}$ are greater than > 0.5 all the way upward from the surface to 20 hPa with confidence levels > 98%, with a maximum correlation of 0.8 at 100–200 hPa. Above 20 hPa however the correlations are small and statistically insignificant.

[25] Given the remarkably high correlations between the P_{swDJ} and the middle to late winter averaged NAM$_{JFM}$ at HS, and the fact that the NAM describes a large-scale oscillation mode of the NH circulation, it is pertinent to examine how P_{swDJ} may perturb the NH zonal-wind and temperature. Figure 7 shows the correlation, in a latitudinal-altitude cross section, between P_{swDJ} and the deseasonalized January–February mean zonal-mean zonal wind U_{JF} (1st row), and both the deseasonalized January–February mean temperature T_{JF} (2nd row). The 1st, 2nd and 3rd columns are for all data, HS and LS conditions, respectively. Similar but slightly smaller correlation coefficients with less statistical confidence are obtained if the January–March mean wind and temperature are used (not shown).

[26] Significant correlations (with confidence levels >95%) between P_{swDJ} and U_{JF} can be found when all the data are used despite the fact that the correlation coefficients are relatively low ($r < 0.5$). The signals are found primarily in the stratosphere and are characterized by a pair of subtropical and high latitude circulation cells that zonal winds rotate in opposite directions. Positive correlations dominate the region poleward of ∼45°N while negative correlations mark the region of 20–40°N. In temperature, the signals of P_{swDJ} are confined to the extratropics and are manifested by negative correlations in the Arctic upper troposphere and lower stratosphere, and positive correla-

---

Figure 2. Composites of deseasonalized zonal mean zonal wind in units of m s^{-1} (lined contours) and temperature in units of K (color shaded contours) for December to April (from top to bottom) when: P_{sw} is high (left panels); P_{sw} is low (right panels). The composites of December are derived based on December mean P_{sw} while those of January through April are derived based on December–January mean P_{swDJ}. Thick solid lines represent zero wind. The total number of data samples is indicated on the top of each panel. The years belonging to the group of high P_{swDJ} are: 1966, 1972–1979, 1982, 1984–1988, 1990, 1992–1996, and 2005, and the years belonging to the group of low P_{swDJ} are: 1967–1971, 1980, 1981, 1989, 1991, 1997–2004, and 2006. The value of P_{swDJ} is unavailable for 1983. Because of the possible contamination of the two major volcanic eruptions, 1982 (after February), 1984 (before March), 1992, and 1993 are excluded.
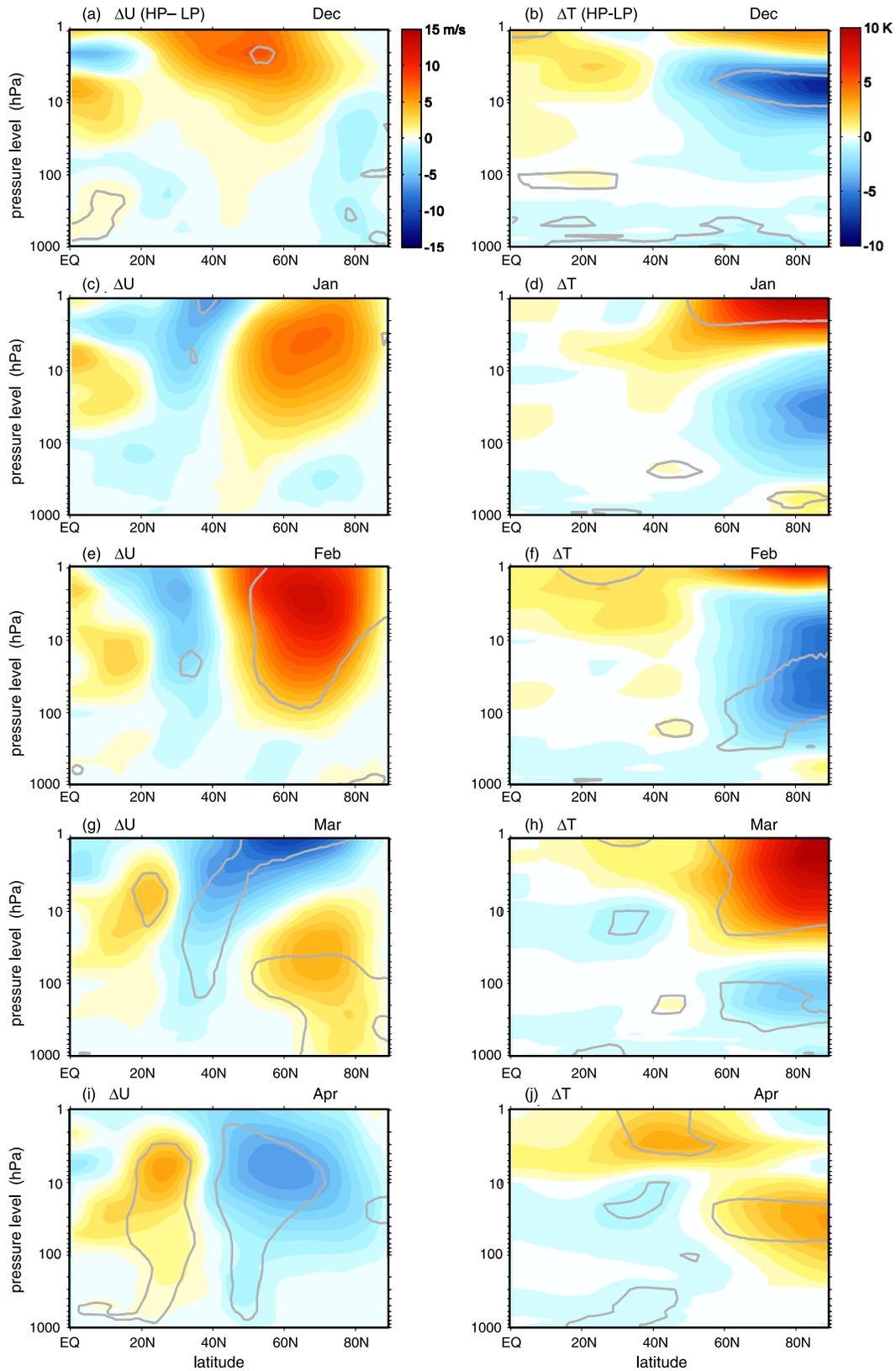
Figure 3. Same as Figure 2, but the composite differences (high P_{swDJ} minus low P_{swDJ}) for zonal–mean zonal wind (left hand panels (a, c, e, g, i)) and temperature (right hand panels (b, d, f, h, j)) from December to April (from top to bottom). The areas enclosed within the gray lines indicate that the differences are statistically significant from zero with a confidence level of 90% or above, calculated using a Monte Carlo trial-based non-parametric test.
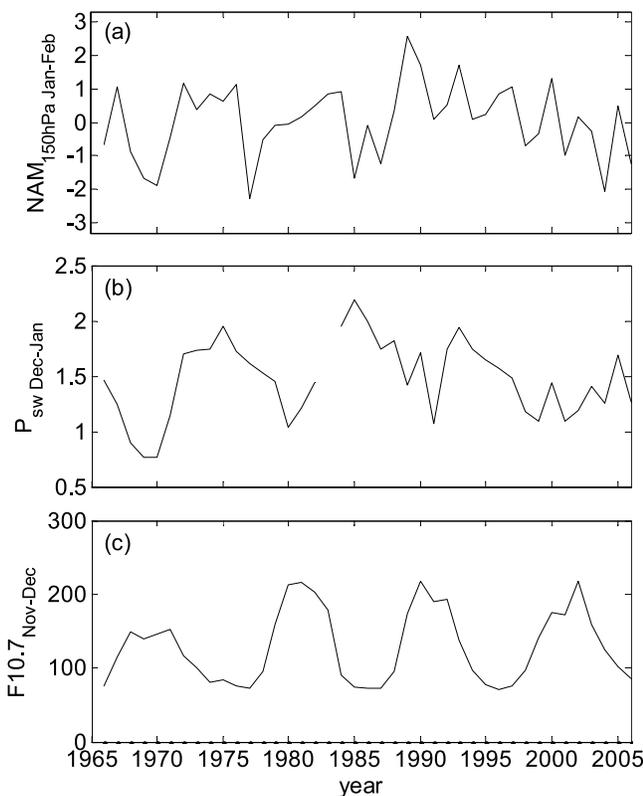
Figure 4. (a) Time series of January–February mean NAM at 150 hPa; (b) Dec-Jan mean P_{swDJ} (in units of 10^{18} n m^{-1} s^{-2}); and (c) November–December mean F10.7 solar flux $F_{s\ ND}$ in solar flux units (1 sfu = 10^{-22} Wm^{-2}Hz^{-1}). Solar wind data is unavailable from December 1982 to January 1983.

tions in the troposphere near $\sim$40–60°N and in the Arctic upper stratosphere.

[27] At HS, qualitatively similar, but much stronger and more robust correlations are obtained. The statistical relationship between P_{swDJ} and U_{JF} are again characterized by positive correlations $\sim$45°N and poleward and negative correlations around $\sim$20–40°N. The correlation coefficient is up to ±0.8 and is highly significant statistically. The P_{swDJ} signals, measured by the light shaded area as having 90% confidence levels and above, extend from the surface to 5 hPa in the polar flank, and from 500 hPa to 2 hPa in the mid-latitude flank. In both flanks, the correlation reaches its maximum at 100–200 hPa with r_{max} = 0.8 and 0.7 respectively, implying that up to 50–65% of the variations in the extratropical monthly mean wind anomalies can be accounted for by P_{swDJ}. In temperature, the signals of P_{swDJ} are manifested by negative correlations in the Arctic upper troposphere and lower stratosphere, positive correlations in the troposphere near $\sim$40–60°N, and negative correlations in the subtropical lower troposphere.

[28] The dynamic implication of those signals is that anomalous rising motion near the Hadley cell and over sub-polar latitudes, and corresponding subsidence at mid-latitudes, occurs under the condition when P_{swDJ} is enhanced. The P_{swDJ} signals in the upper stratosphere are

somehow opposite and marked by positive correlations in the Arctic and negative correlations in the extra-polar region. Positive correlations in temperature are observed near the tropical tropopause region, though these correlations are not significant. Nevertheless, the out-of-phase relationship between lower stratospheric temperature anomalies at tropical and polar latitudes reflects adiabatic temperature changes induced by a weakening of the BD circulation in the lower stratosphere. Overall, these P_{swDJ} signals in U_{JF} and T_{JF} are remarkably similar to those of the NAM [*Baldwin and Dunkerton*, 2001; *Thompson et al.*, 2003], explaining the significant correlations between P_{swDJ} and the NAM $_{JF}$ shown in Figure 6. No significant correlations can be found in either U_{JF} or T_{JF} at LS.

[29] Figure 8 shows the correlation between P_{swDJ} and January–February mean U_{JF} extracted at 60°N, 150 hPa (left panel), and January–February mean T_{JF} at 80°N, 200 hPa (right panel), at HS. Strikingly clear positive and negative correlations are shown for U_{JF} and T_{JF}, respectively, suggesting that a colder and stronger lower stratospheric polar vortex is present when P_{swDJ} is high. At those locations, the maximum differences are up to 14 m s^{-1} in U_{JF} and 12 K in T_{JF}.

[30] A remaining issue is whether there is no response in the stratosphere and troposphere to solar wind forcing at LS at all or whether the response is delayed and hence does not reveal itself in the analysis reported above. We can check this by repeating the same analysis with a delay between the solar wind forcing parameter P_{swDJ} and the atmospheric variables U, T and the NAM. Figure 9 shows the correlations, in a latitudinal altitude cross-section, between P_{swDJ} and the deseasonalized Mar-Apr mean zonal-mean zonal wind U_{MA} (upper panel), and temperature T_{MA} (lower panel) at LS. It shows that significant correlations (measured by the confidence levels >90%) are now apparent between P_{swDJ} and U_{MA}; these are mostly confined to the extratropics. The signals are characterized by negative correlations poleward of $\sim$45°N in the stratosphere, and positive correlations in the Arctic troposphere. The maximum correlation coefficient r_{max} reaches 0.67 at 75°N, 700 hPa (also see Figure 10a). The corresponding signals of P_{swDJ} in T_{MA} are mostly confined to the Arctic and are marked by positive correlations in the lower to middle stratosphere and negative correlations in the troposphere. Negative correlations in temperature are apparent near the tropical tropopause. Though the tropical correlations are not statistically significant, the out-of-phase relationship between lower stratospheric temperature correlations at tropical and polar latitudes reflects adiabatic temperature changes induced by a strengthened BD circulation. The maximum correlation coefficient r_{max} reaches 0.66 at 80°N, 800 hPa, suggesting that P_{swDJ} accounts for up to 40% of monthly mean temperature variations in the Arctic lower troposphere (see Figure 10b). Figure 10 shows that, at LS, the associated maximum differences in tropospheric wind and temperature are up to 5 m s^{-1} and 3 K, respectively.

[31] Figure 11 shows the correlations between P_{swDJ} and the March mean ERA40-NAM at LS. It shows that significant negative correlations between P_{swDJ} and March mean NAM exist in the stratosphere and the correlation peaks at $\sim$7 hPa with r_{min} = −0.65. No significant correlation is
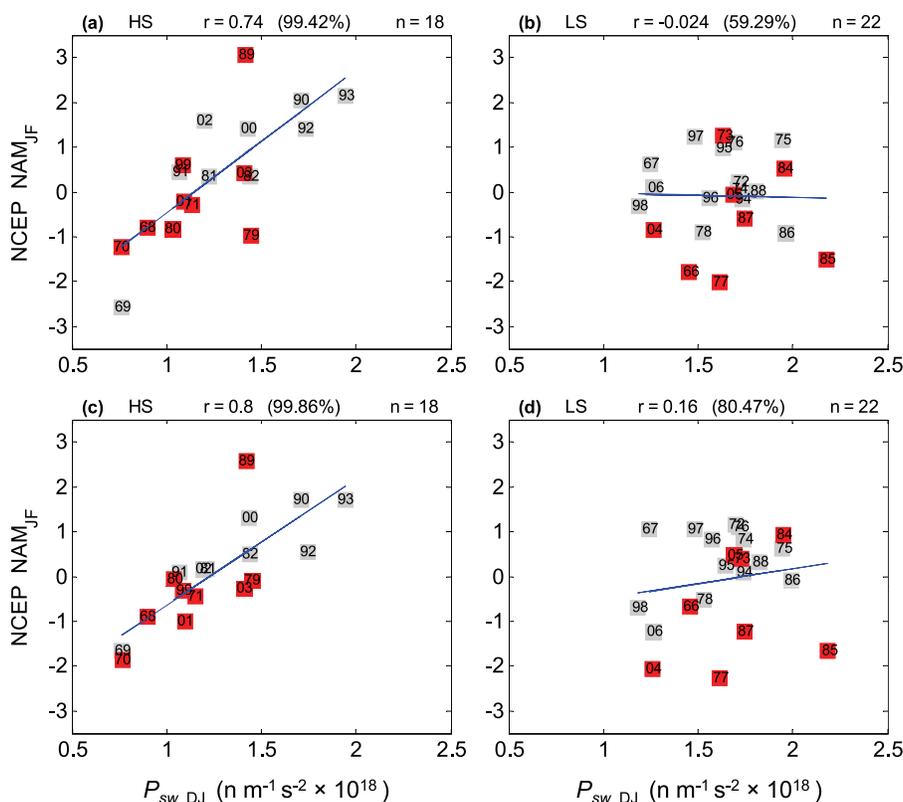
Figure 5. Correlation between P_{swDJ} and January–February mean NCEP-NAM at 150 hPa at HS (a) and LS (b). (c) and (d) are the same as (a) and (b) but use NAM derived from blended ECMWF ERA-40 and Operational data. The years belonging to the group of HS are: 1968–1971, 1979–1983, 1989–1992, and 1999–2003 and the years belonging to the group of LS include: 1966, 1967, 1972– 1978, 1984–1988, 1994–1998, and 2004–2006. The data are shown in actual years with two-digit numbering, and a solid line shows the linear regression to the data. The red shaded data indicate a major stratospheric sudden warming (SSW) event has occurred during January and February in the year.

found in the troposphere, presumably implying a lack of coupling from the stratosphere to the troposphere.

4. Discussions

[32] Recent modeling studies have shown complex dynamic linkages between stratospheric forcing and changes in tropospheric eddy activity [*Limpasuvan and Hartmann*, 2000; *Kushner and Polvani*, 2004; *Gerber and Vallis*, 2007]. It has been found that as the polar winter stratosphere is cooled, the tropospheric jet shifts poleward and the dynamic response projects almost entirely and positively onto the annular mode [*Kushner and Polvani*, 2004; *Haigh and Blackburn*, 2005]. At the same time, the vertical flux of wave activity from the troposphere to the stratosphere is reduced, and the meridional flux of wave activity from high to low latitudes is increased. Thus the stratospheric wave drag is reduced if the polar upper stratosphere is anomalously cooler. Shown in Figures 2 and 7, in winter, an anomalously stronger and colder polar vortex is associated with HP, while a weaker and warmer polar vortex is associated with LP. Such effects start in December in the upper stratosphere and last until February to March. The zonal wind response to enhanced solar wind forcing is broadly similar to the results of *Kushner and Polvani* [2004] who modeled the stratosphere and troposphere

responses to the impacts of polar upper stratospheric cooling. This implies anomalous cooling or reduced wave forcing in the stratosphere under HP. The poleward and downward migration of the solar wind signature from the upper stratosphere to the troposphere further indicates that the solar wind perturbation on stratospheric circulation is manifested primarily through changes in the wave-meanflow interaction [*Kuroda and Kodera*, 1999, 2004].

[33] Possible solar UV perturbations on the NAM have been interpreted in relation to the structure of the polar vortex and its ability to refract the upward propagating planetary waves [*Kodera and Kuroda*, 2005]. At HS, the changes in the mean flow occurring in the upper stratosphere favor more planetary waves to be deflected/suppressed. According to the "downward control" principle [*Haynes et al.*, 1991], by redistributing the angular momentum, it further affects the wave forcing on the meanflow at the lower levels. *Kodera and Kuroda* [2005] suggested that the more zonally symmetric pattern of the NAO at HS is a result of prolonged downward extension of solar-induced wind anomalies. Here we show that the seasonal progression of HP composites shows a degree of similarity to that of HS composites previously reported by *Kodera and Kuroda* [2002, 2005]. For both cases, the response to solar forcing is characterized by a poleward and downward jet
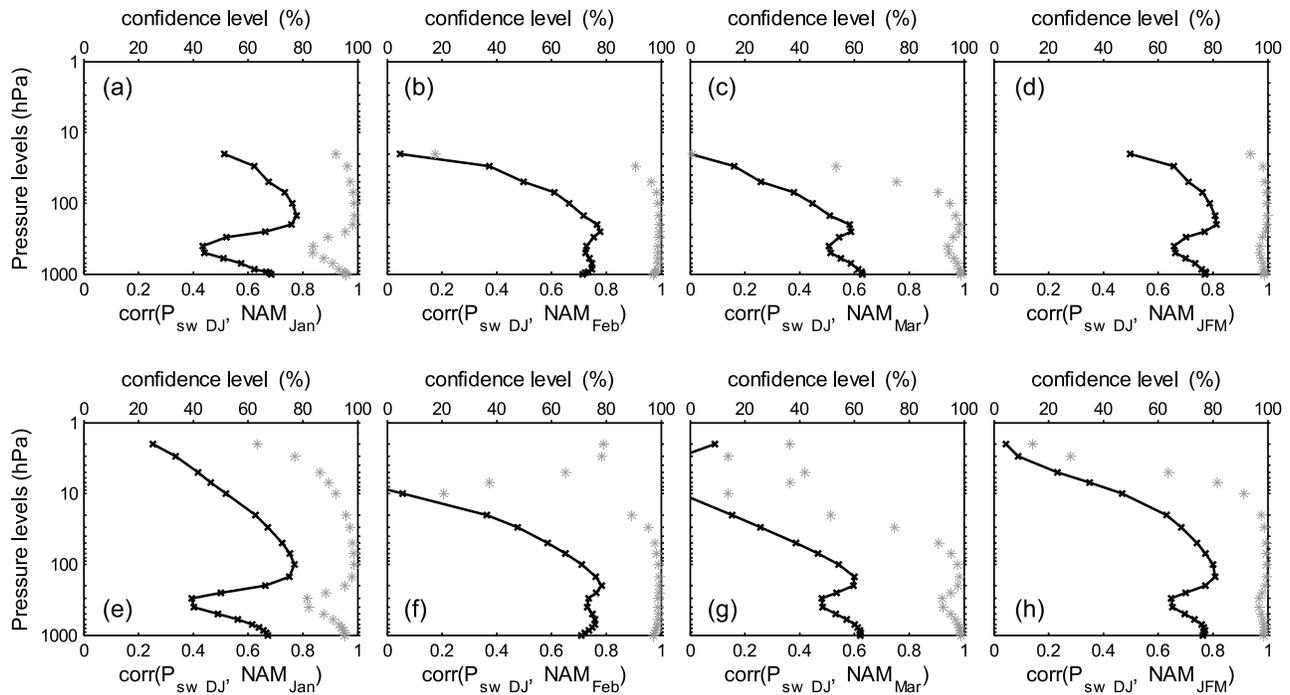
Figure 6. From (a) to (d): correlation coefficients (black solid lines with crosses) and confidence levels in percentage unit (gray star) between Dec-Jan mean P_{swDJ} and January, February, March, and the three-month mean NCEP-NAM (from top to bottom) with 17 pressure levels from 1000-10 hPa at HS. From (e) to (h): same as (a) to (d) but using ERA-40 Reanalysis derived NAM with 23 pressure levels from 1000 to 1 hPa. For all the cases, the sampling years are the same as those in Figure 5 at HS.
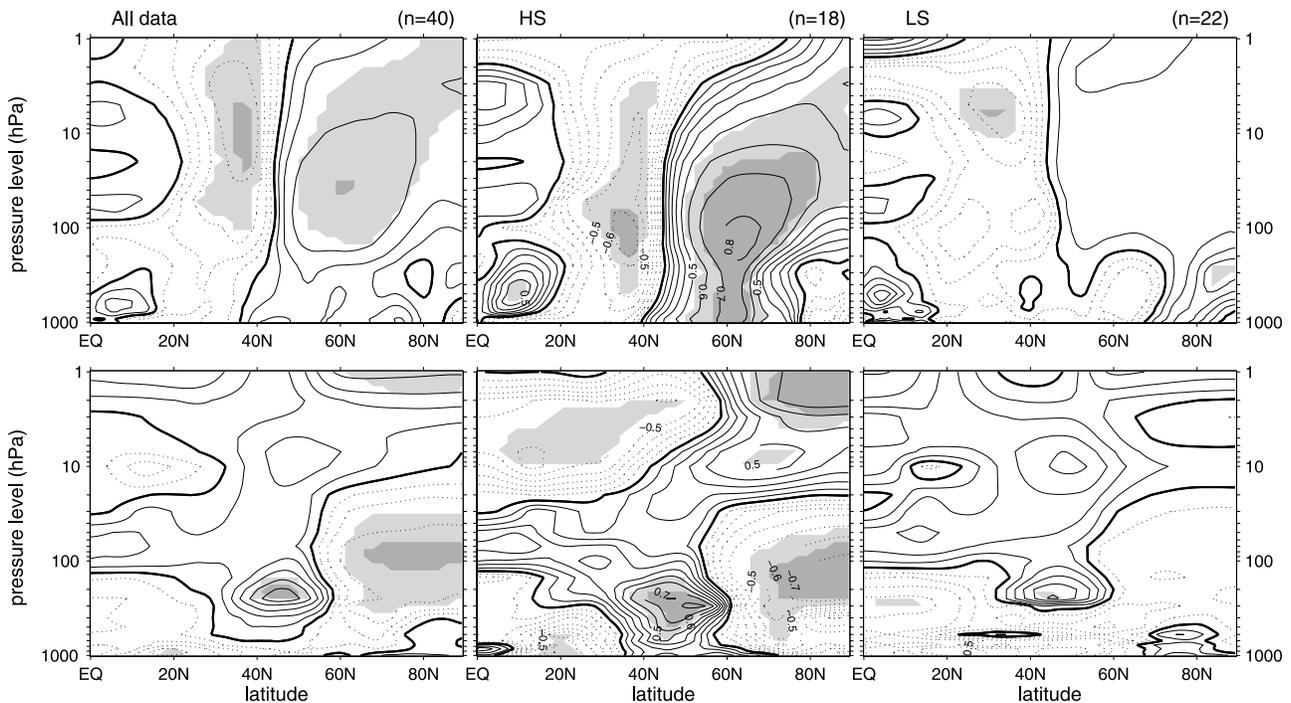

Figure 7. Linear correlations between December and January mean P_{swDJ} and deseasonalized January–February averaged zonal mean zonal wind U_{JF} (1st row), and temperature $\underline{T}_{JF}$ (2nd row), under all data (1st column), HS (i.e. $F_{sND} > \overline{F_{sND}}$) (2nd column), and LS (i.e. $F_{sND} < \overline{F_{sND}}$) (3rd column). Contour interval is ±0.1 and the thick black contour is zero correlation. The light and dark gray shaded areas indicate that the correlations are statistically significant at confidence levels greater than 90% and 95%, respectively. The sampling years are those shown in Figure 5.
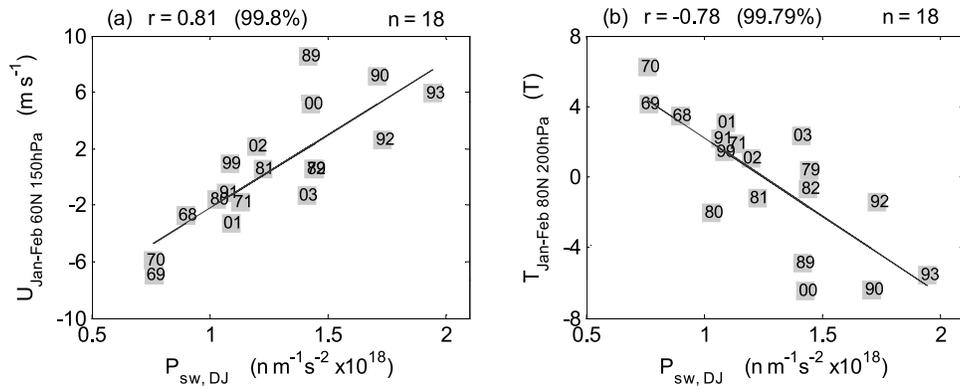
Figure 8. Same as Figures 3a and 3c, but for the correlations between $P_{sw\mathrm{DJ}}$ and deseasonalized January–February mean wind U_{JF} at 60°N, 150 hPa (a) and temperature T_{JF} at 80°N, 200 hPa (b) at HS. The data samples are the same as those in the left-hand panels of Figure 5 and are shown in years with two-digit numbering. The solid lines show the linear regression to the data.

shift. While stronger solar UV forcing is likely to result in a weaker polar vortex [*Kodera and Kuroda*, 2002], enhanced solar wind forcing seems to give rise to a stronger and colder polar vortex in middle to late winter. In contrast, enhanced solar wind forcing seems to persistently cool and strengthen the polar vortex in mid- to late winter.

[34] *Castanheira and Graf* [2003] showed that the state of the stratospheric polar vortex affects the correlation between the NAO and the sea level pressure. The correlations are confined to the Atlantic sector under a weak polar vortex, whereas under a strong polar vortex, the correlations extend to the North Pacific. Here we show that statistically significant correlations between the NAM and $P_{sw\mathrm{DJ}}$ exist when early winter solar irradiance flux is anomalously high. HP gives rise to a cooler polar upper stratosphere (see Figure 2a) and enhances the equator to pole temperature gradient. Such solar wind induced thermal perturbations in the upper stratosphere can be further enhanced at HS [*Kodera and Kuroda*, 2002] and cause stronger, detectable responses in the lower levels. This is probably why the spatial pattern of the winter NAM was confined to the Atlantic sector at LS, whereas it showed a hemispherical structure at HS [*Kodera*, 2002, 2003].

[35] By using a middle atmospheric GCM, *Arnold and Robinson* [1998] demonstrated that, in the winter hemisphere, the 11-yr SC modulation of planetary wave propagation reinforces thermal perturbations in the thermosphere. They suggested that, through wave-meanflow interaction, upward propagating planetary waves can couple solar-induced changes in the thermosphere down to the stratosphere and lead to changes in the middle atmosphere circulation. The effect is marked by a weakened polar wind and a strengthened wind at mid-latitudes at HS. *Arnold and Robinson* [2001] extended this work to show that the heating induced by solar wind driven magnetic flux could also produce a measurable stratospheric response without incorporating any external forcing within the stratosphere. The effect is marked by a stronger and colder polar vortex under high geomagnetic activity. Thus the results shown in Figure 2 seem to support the mechanism proposed by *Arnold and Robinson* [2001].

[36] Apart from dynamic transfer of solar forcing, solar wind disturbances may be transferred downward through changes in chemical constituents via energetic particle precipitation (EPP) [*Solomon et al.*, 1982]. Odd nitrogen NO_x ($NO + NO_2$) generated by EPP during geomagnetic storms can descend from the upper mesosphere and the lower thermosphere into the stratosphere during polar winter and spring [*Callis et al.*, 1991; *Siskind et al.*, 2000; *Callis*, 2001; *Randall et al.*, 2005; *Seppälä et al.*, 2007], and may affect the stratospheric radiative balance through cat-
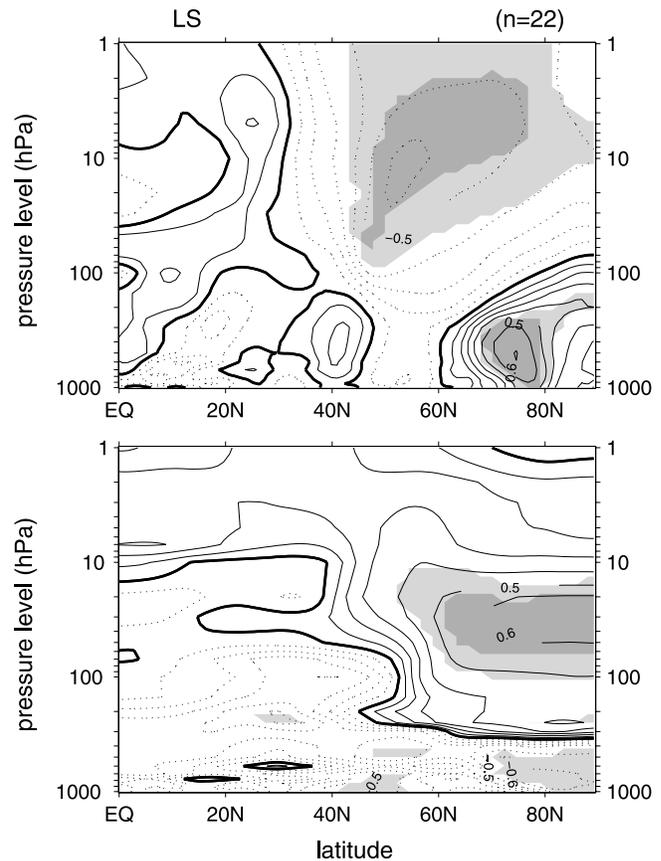

Figure 9. Same as the 3rd column of Figure 7, except that the deseasonalized zonal wind and temperature are replaced by the March to April mean U_{MA} and T_{MA}.
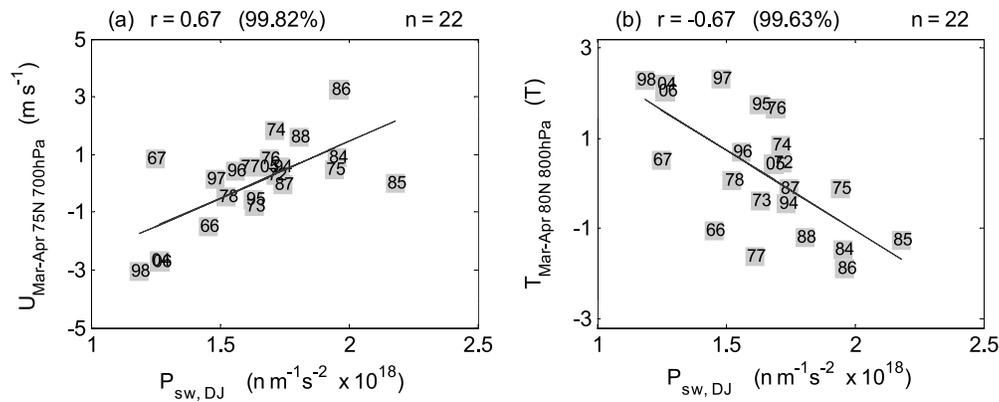
Figure 10. Same as Figure 8, except that the zonal wind in (a) is the de-seasonalized March−April mean at 75°N, 700 hPa, and the temperature (b) is the de-seasonalized March−April mean at 80°N, 800 hPa in the Arctic troposphere at LS. The data samples are the same as those in the right-hand panels of Figure 5 and are shown in years with two-digit numbering. The solid lines show the linear regression to the data.

alytic reactions [*Brasseur and Solomon*, 2005]. The NO_x, transported downward from high altitudes by the polar vortex, would typically take 1−3 months to reach the upper stratosphere and hence stratospheric responses are likely to take place in spring [*Siskind et al.*, 2000]. Thus the rather instantaneous cooling responses in winter months to solar wind dynamic pressure seem to rule out the possibility of chemical forcing in the stratosphere by EPP-NO_x. If the chemical responses are through a simple local cooling effect of *in situ* chemistry between stratospheric O_3 and descending high-altitude EPP-NO_x, it is expected that the response to the EPP induced NO_x should be a cooling of the polar upper stratosphere because of the loss of O_3 and consequent reduction in solar UV absorption. However the dominant feature of spring polar stratospheric temperature response to $P_{sw\ DJ}$ is warming rather than cooling. This is similar to what has been found by *Lu et al.* [2008b], who used geomagnetic Ap index to represent EPP induced NO_x and discovered warming, rather than cooling, responses in the polar stratospheric temperature. They suggested that the stratospheric temperature responses to geomagnetic perturbations are likely to be indirect and of dynamic origin. Nevertheless, more detailed radiation budget estimations are required before a concrete conclusion can be made.

[37] In early winter and at HS, the equator to pole temperature gradient in the upper stratosphere increases, and results in an anomalously weaker polar vortex [*Kodera and Kuroda*, 2002]. This further increases the equator to pole temperature gradient in the lower stratosphere. *Haigh* [1996] suggested that an increase in stratospheric temperature due to UV heating at HS leads to a strengthening of easterly winds penetrating into the troposphere near the subtropics, consequently altering the circulation near the surface. The dynamic consequence is that the tropospheric mid-latitude jet is displaced poleward and the planetary waves propagating from the troposphere into the stratosphere are shifted poleward [*Haigh*, 1999; *Haigh and Blackburn*, 2005]. Such a change in the mean tropospheric circulation allows more planetary waves to travel equatorward and less planetary waves to travel poleward. Less planetary wave forcing in the polar stratospheric region

means a stronger and colder polar vortex. The combined effect of high solar UV irradiance and high P_{sw} in the NH winter is even stronger westerlies in the extratropics and weaker westerlies in the subtropics, which refract more planetary waves toward the equator. It is known that anomalies in both tropospheric and stratospheric circulation influence the probability of planetary wave propagation [*Limpasuvan and Hartmann*, 2000]. When the planetary waves are shifted poleward near the tropopause because of the enhanced solar UV forcing, the wave-meanflow interaction is characterized by enhanced positive feedback to changes of the equator to pole temperature gradient in the upper stratosphere, and this effect is mostly projected onto the NAM [*Kushner and Polvani*, 2004; *Song and Robinson*, 2004]. Thus the changes in the background circulation by solar UV may provide a suitable wave-guide condition for stratospheric solar wind forcing signals to be extended downward. Thus the sensitivity of planetary wave propagation in winter to the background temperature and wind structure provides a possible mechanism by which the solar
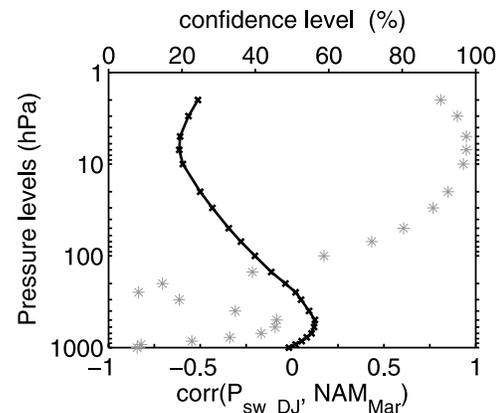

Figure 11. Correlation coefficients (black solid lines with crosses) and confidence levels in percentage unit (gray stars) between $P_{sw DJ}$ and ERA-40 Reanalysis derived NAM for March at LS. The sampling years are the same as those in the right hand panels of Figure 5.

wind influences penetrate from the upper stratosphere to the troposphere. Although these mechanisms might explain the robustly high correlations between P_{swDJ} and the January–March mean NAM, the precise details of how that influence is achieved are unknown.

[38] During the NH winter, the quasi-biennial oscillation (QBO) in the equatorial lower stratosphere strongly influences the polar stratosphere. The well-known phenomenon often referred to as the Holton–Tan (HT) effect, suggests a colder and stronger polar vortex during westerly QBO, and a warmer and more disturbed polar vortex during easterly QBO [*Holton and Tan*, 1980, 1982]. Studies have noted that the HT effect is strongest when the 11-yr solar cycle is at its minimum but that the relationship substantially weakens or even reverses during solar maximum [*Labitzke and Chanin*, 1988; *Naito and Hirota*, 1997; *Gray et al.*, 2001]. Here we find that the Arctic stratospheric temperature is strongly correlated with P_{swDJ} during HS winter. Compared to the QBO signals in the extratropical stratosphere extracted from the same data set [*Lu et al.*, 2008a], the magnitude of the P_{swDJ} signals in winter months are larger than that of the QBO. This may be one explanation of why the HT effect has been found to be substantially weaker around solar maximum.

5. Conclusions

[39] In the NH winter, the response of atmospheric circulation to solar wind dynamic pressure enhancement appears to be marked by a stronger polar vortex and a weaker sub-tropical jet in the upper to middle stratosphere. Westerly anomalies appear in the subtropics to mid-latitudes near the stratopause in December. Then the subtropical jet becomes weaker and the polar vortex becomes stronger in January through March. As the winter progresses, the Arctic becomes colder and the jet anomalies shift poleward and downward.

[40] There are substantial differences between the signals of solar wind dynamic pressure P_{swDJ} at HS and those at LS. At HS, P_{swDJ} is positively correlated with the January to March NAM all the way from the surface to the mid-stratosphere, except for the pressure levels between 300 and 500 hPa. This implies a strengthened polar vortex, a reduced Brewer–Dobson circulation and enhanced coupling between the stratosphere and the troposphere. The signature of P_{swDJ} is marked by an oscillation pattern with westerly anomalies at ~40–80°N, extending from the surface to the 10 hPa pressure level, and easterly anomalies at ~20–40°N, extending from 500 hPa to 2 hPa. The corresponding signals in temperature are marked by out-of-phase relationships of temperature anomalies both between low and high latitudes and between the stratosphere and troposphere. In the polar region, it is characterized by a vertical bipolar structure with warming in the upper stratosphere and cooling in the lower stratosphere and troposphere. The opposite pattern holds at sub-tropical to mid-latitudes.

[41] At LS, there is no signature of P_{swDJ} in the NH winter but negative correlations between P_{swDJ} and the NAM are found in the stratosphere during spring (i.e., March and April), implying a delayed and opposite solar wind perturbation on the stratospheric circulation compared

to those occurring in winter at HS. The correlation between P_{swDJ} and the NAM is highly significant. The spatial patterns of P_{swDJ} signature in zonal wind and temperature are remarkably robust and are consistent with the known pattern of the NAM in zonal wind and temperature. In spring, the wind and temperature responses to P_{swDJ} are confined to high latitudes and there is no correlation with the NAM in the troposphere, suggesting a hampered stratosphere-troposphere coupling compared to that under HS conditions.

[42] We note that, for the period from 1966–2006, both the magnitudes of P_{swDJ} signals and the correlation coefficients are larger than those associated with the 11-yr SC and the QBO. The results suggest that, in addition to solar UV irradiance, solar wind may also play a significant role in perturbing large-scale circulation in the stratosphere and troposphere. Despite the statistical robustness of the P_{swDJ} signals, they do not explain the mechanism by which variations in the upper stratospheric wind and temperature are influenced by the solar wind dynamic pressure. We speculate that possible mechanisms could be:

[43] 1. geomagnetic activity induced chemical changes, such as NO_x enhancement, and their downward descent under dark polar vortex conditions may be enhanced by solar UV heating of O_3 in the stratosphere; this indirectly strengthens the polar vortex transporting NO_x-rich air into the upper stratosphere [*Randall et al.*, 2005];

[44] 2. temperature changes induced by solar wind forcing in the mesosphere and the lower thermosphere cause changes in the waveguides of the upward propagating waves [*Arnold and Robinson*, 1998, 2001].

[45] These two mechanisms may work in combination but more studies are needed to identify the actual mechanisms. However we note that given the relatively short response time and inactiveness of the stratospheric catalytic reaction cycles in the winter polar region, it is unlikely that the *in situ* chemical effect of descending EPP-NO_x on stratospheric ozone would have a dominant influence on the strengthening of the polar vortex [*Lu et al.*, 2008b].

[46] The route by which the effects of either solar irradiance or solar wind forcing might propagate to the lower atmosphere is yet to be explored. The results reported here strongly indicate complex dynamic interactions between the two different types of solar forcing. Previously reported mechanisms in terms of stratosphere-troposphere coupling may be used to explain such interactions [*Kushner and Polvani*, 2004; *Song and Robinson*, 2004; *Haigh et al.*, 2005; *Haigh and Blackburn*, 2005]. Nevertheless, the 11-yr SC modulated P_{swDJ} signals found in the observational data are intriguing. Further studies are required to understand how enhanced solar wind forcing modulates the upward propagating planetary waves, and why the modulation differs from solar maximum to solar minimum. Studies are also needed to understand in detail why there is a stronger stratosphere-troposphere coupling of P_{swDJ} signals (through the NAM) at HS and why the P_{swDJ} signals are opposite and delayed at LS. A satisfactory explanation for such multiple solar influences must address two questions: Firstly, how and to what extent do solar UV and solar wind related processes impact on the variations in the stratospheric zonal flow and temperature? Secondly, how and to what extent do such modulations of the stratospheric mean

circulation affect the amplitude and location of stratospheric wave drag and the associated radiative heating? In addition, more studies are needed to determine to what extent the processes occurring in the mesosphere and the thermosphere influence the circulation in the lower part of the atmosphere.

References

Arnold, N. F., and T. R. Robinson (1998), Solar cycle changes to planetary wave propagation and their influence on the middle atmosphere circulation, *Ann. Geophys.*, 16, 69–76.

Arnold, N. F., and T. R. Robinson (2001), Solar magnetic flux influences on the dynamics of the winter middle atmosphere, *Geophys. Res. Lett.*, 28, 2381–2384.

Austin, J., L. L. Hood, and B. E. Soukharev (2007), Solar cycle variations of stratospheric ozone and temperature in simulations of a coupled chemistry-climate model, *Atmos. Chem. Phys.*, 7, 1693–1706.

Baldwin, M. P. (2001), Annular modes in global daily surface pressure, *Geophys. Res. Lett.*, 28, 4115–4118.

Baldwin, M. P., and T. J. Dunkerton (1999), Propagation of the Arctic Oscillation from the stratosphere to the troposphere, *J. Geophys. Res.*, 104, 30,937–30,946.

Baldwin, M. P., and T. J. Dunkerton (2001), Stratospheric harbingers of anomalous weather regimes, *Science*, 294, 581–584.

Boberg, F., and H. Lundstedt (2002), Solar wind variations related to fluctuations of the North Atlantic Oscillation, *Geophys. Res. Lett.*, 29(15), 1718, doi:10.1029/2002GL014903.

Boberg, F., and H. Lundstedt (2003), Solar wind electric field modulation of the NAO: A correlation analysis in the lower atmosphere, *Geophys. Res. Lett.*, 30(15), 1825, doi:10.1029/2003GL017360.

Bochnicek, J., and P. Hejda (2005), The winter NAO pattern changes in association with solar and geomagnetic activity, *J. Atmos. Sol. Terr. Phys.*, 67, 17–32.

Boudouridis, A., E. Zesta, L. R. Lyons, P. C. Anderson, and D. Lummerzheim (2003), Effect of solar wind pressure pulses on the size and strength of the auroral oval, *J. Geophys. Res.*, 108(A4), 8012, doi:10.1029/2002JA009373.

Brasseur, G., and S. Solomon (2005), *Aeronomy of the Middle Atmosphere*, 3rd ed., Springer, Dordrecht, Netherlands.

Bucha, V., and V. Bucha (1998), Geomagnetic forcing of changes in climate and in the atmospheric circulation, *J. Atmos. Sol. Terr. Phys.*, 60, 145–169.

Callis, L. B. (2001), Stratospheric studies consider crucial question of particle precipitation, *Eos Trans. AGU*, 82, 297.

Callis, L. B., R. E. Boughner, M. Natarajan, J. D. Lambeth, D. N. Baker, and J. B. Blake (1991), Ozone depletion in the high-latitude lower stratosphere—1979–1990, *J. Geophys. Res.*, 96, 2921–2937.

Camp, C. D., and K. K. Tung (2007), Surface warming by the solar cycle as revealed by the composite mean difference projection, *Geophys. Res. Lett.*, 34, L14703, doi:10.1029/2007GL030207.

Castanheira, J. M., and H.-F. Graf (2003), North Pacific–North Atlantic relationships under stratospheric control?, *J. Geophys. Res.*, 108(D1), 4036, doi:10.1029/2002JD002754.

Crooks, S. A., and L. J. Gray (2005), Characterization of the 11-year solar signal using a multiple regression analysis of the ERA-40 dataset, *J. Clim.*, 18, 996–1015.

Davis, R. E. (1976), Predictability of sea surface temperature and sea level pressure anomalies over the North Pacific Ocean, *J. Phys. Oceanogr.*, 6, 249–266.

Finch, I., and M. Lockwood (2007), Solar wind-magnetosphere coupling functions on timescales of 1 day to 1 year, *Ann. Geophys.*, 25, 495–506.

Gerber, E. P., and G. K. Vallis (2007), Eddy-zonal flow interactions and the persistence of the zonal index, *J. Atmos. Sci.*, 64, 3296–3311.

Gimeno, L., L. de la Torre, R. Nieto, R. García, E. Hernández, and P. Ribera (2003), Changes in the relationship NAO-Northern hemisphere temperature due to solar activity, *Earth Planet. Sci. Lett.*, 206, 15–20.

Gray, L. J., S. J. Phipps, T. J. Dunkerton, M. P. Baldwin, E. F. Drysdale, and M. R. Allen (2001), A data study of the influence of the equatorial upper stratosphere on northern-hemisphere stratospheric sudden warmings, *Q. J. R. Meteorol. Soc.*, 127, 1985–2003.

Haigh, J. D. (1994), The role of stratospheric ozone in modulating the solar radiative forcing of climate, *Nature*, 370, 544–546.

Haigh, J. D. (1996), The impact of solar variability on climate, *Science*, 272, 981–984.

Haigh, J. D. (1999), A GCM study of climate change in response to the 11-year solar cycle, *Q. J. R. Meteorol. Soc.*, 125, 871–892.

Haigh, J. D. (2003), The effects of solar variability on the Earth's climate, *Philos. Trans. R. Soc. London, Ser. A-Math. Phys. Eng. Sci.*, 361, 95–111.

Haigh, J. D., and M. Blackburn (2005), Solar influences on dynamical coupling between the stratosphere and troposphere, *Space Sci. Rev.*, 125, 331–344.

Haigh, J. D., M. Blackburn, and R. Day (2005), The response of tropospheric circulation to perturbations in lower stratospheric temperature, *J. Clim.*, 18, 3672–3691.

Haynes, P. H., C. J. Marks, M. E. McIntyre, T. G. Shepherd, and K. P. Shine (1991), On the "downward control" of extratropical diabatic circulations by eddy-induced mean zonal forces, *J. Atmos. Sci.*, 48, 651–679.

Holton, J. R., and H. C. Tan (1980), The influence of the equatorial quasi-biennial oscillation on the global circulation at 50 mb, *J. Atmos. Sci.*, 37, 2200–2208.

Holton, J. R., and H. C. Tan (1982), The quasi-biennial oscillation in the Northern Hemisphere lower stratosphere, *J. Meteorol. Soc. Japan*, 60, 140–148.

Hood, L. L. (2004), Effects of solar UV variability on the stratosphere, in *Solar Variability and its Effect on the Earth.s Atmosphere and Climate System*, Monogr. Ser., vol. 141, edited by J. Pap et al., 283–303, AGU, Washington, D. C.

Hoyt, D. V., and K. H. Schatten (1997), *The Role of the Sun in Climate Change*, 288 pp., Oxford Univ. Press, New York.

Hurrell, J. W. (1995), Decadal trends in the north-Atlantic oscillation—Regional temperatures and precipitation, *Science*, 269, 676–679.

King, J. H., and N. E. Papitashvili (2005), Solar wind spatial scales in and comparisons of hourly wind and ACE plasma and magnetic field data, *J. Geophys. Res.*, 110, A02104, doi:10.1029/2004JA010649.

Kodera, K. (2002), Solar cycle modulation of the North Atlantic Oscillation: Implication in the spatial structure of the NAO, *Geophys. Res. Lett.*, 29(8), 1218, doi:10.1029/2001GL014557.

Kodera, K. (2003), Solar influence on the spatial structure of the NAO during the winter 1900–1999, *Geophys. Res. Lett.*, 30(4), 1175, doi:10.1029/2002GL016584.

Kodera, K., and Y. Kuroda (2002), Dynamical response to the solar cycle, *J. Geophys. Res.*, 107(D24), 4749, doi:10.1029/2002JD002224.

Kodera, K., and Y. Kuroda (2005), A possible mechanism of solar modulation of the spatial structure of the North Atlantic Oscillation, *J. Geophys. Res.*, 110, D02111, doi:10.1029/2004JD005258.

Kuroda, Y., and K. Kodera (1999), Role of planetary waves in the stratosphere–troposphere coupled variability in the Northern Hemisphere winter, *Geophys. Res. Lett.*, 26, 2375–2378.

Kuroda, Y., and K. Kodera (2004), Role of the polar-night jet oscillation on the formation of the Arctic Oscillation in the Northern Hemisphere winter, *J. Geophys. Res.*, 109, D11112, doi:10.1029/2003JD004123.

Kushner, P. J., and L. M. Polvani (2004), Stratosphere-troposphere coupling in a relatively simple AGCM: The role of eddies, *J. Clim.*, 17, 629–639.

Labitzke, K., and M. L. Chanin (1988), Changes in the middle atmosphere in winter related to the 11-year solar-cycle, *Ann. Geophys.*, 6, 643–644.

Labitzke, K., and H. van Loon (1988), Associations between the 11-year solar-cycle, the QBO and the atmosphere 1. The troposphere and stratosphere in the Northern Hemisphere in winter, *J. Atmos. Sol. Terr. Phys.*, 50, 197–206.

Labitzke, K., M. Kunze, and S. Bronnimann (2006), Sunspots, the QBO and the stratosphere in the North Polar Region—20 years later, *Meteorol. Zeitschrift*, 15, 355–363.

Laundal, K. M., and N. Østgaard (2008), Persistent global proton aurora caused by high solar wind dynamic pressure, *J. Geophys. Res.*, 113, A08231, doi:10.1029/2008JA013147.

Lean, J. L., G. J. Rottman, H. L. Kyle, T. N. Woods, J. R. Hickey, and L. C. Puga (1997), Detection and parameterization of variations in solar mid- and near-ultraviolet radiation (200–400 nm), *J. Geophys. Res.*, 102, 29,939–29,956.

Limpasuvan, V., and D. L. Hartmann (2000), Wave-maintained annular modes of climate variability, *J. Clim.*, 13, 4414–4429.

Liou, K., P. T. Newell, T. Sotirelis, and C.-I. Meng (2006), Global auroral response to negative pressure impulses, *Geophys. Res. Lett.*, 33, L11103, doi:10.1029/2006GL025933.

Liou, K., P. T. Newell, J.-H. Shue, C.-I. Meng, Y. Miyashita, H. Kojima, and H. Matsumoto (2007), "Compression aurora": Particle precipitation driven by long-duration high solar wind ram pressure, *J. Geophys. Res.*, 112, A11216, doi:10.1029/2007JA012443.

Lu, G., T. G. Onsager, G. Le, and C. T. Russell (2004), Ion injections and magnetic field oscillations near the high-latitude magnetopause asso-

ciated with solar wind dynamic pressure enhancement, *J. Geophys. Res.*, *109*, A06208, doi:10.1029/2003JA010297.

Lu, H., M. J. Jarvis, H. F. Graf, P. C. Young, and R. B. Horne (2007), Atmospheric temperature response to solar irradiance and geomagnetic activity, *J. Geophys. Res.*, *112*, D11109, doi:10.1029/2006JD007864.

Lu, H., M. P. Baldwin, L. J. Gray, and M. J. Jarvis (2008a), Decadal-scale changes in the effect of the QBO on the northern stratospheric polar vortex, *J. Geophys. Res.*, *113*, D10114, doi:10.1029/2007JD009647.

Lu, H., M. A. Clilverd, A. Seppälä, and L. L. Hood (2008b), Geomagnetic perturbations on stratospheric circulation in late winter and spring, *J. Geophys. Res.*, *113*, D16106, doi:10.1029/2007JD008915.

Matthes, K., U. Langematz, L. L. Gray, K. Kodera, and K. Labitzke (2004), Improved 11-year solar signal in the Freie Universität Berlin Climate Middle Atmosphere Model (FUB-CMAM), *J. Geophys. Res.*, *109*, D06101, doi:10.1029/2003JD004012.

Matthes, K., Y. Kuroda, K. Kodera, and U. Langematz (2006), Transfer of the solar signal from the stratosphere to the troposphere: Northern winter, *J. Geophys. Res.*, *111*, D06108, doi:10.1029/2005JD006283.

Mayaud, P. N. (1980), *Derivation, Meaning, and Use of Geomagnetic Indices*, AGU, Washington, D. C.

Naito, Y., and I. Hirota (1997), Interannual variability of the northern winter stratospheric circulation related to the QBO and the solar cycle, *J. Meteorol. Soc. Japan*, *75*, 925–937.

Ogi, M., K. Yamazaki, and Y. Tachibana (2003), Solar cycle modulation of the seasonal linkage of the North Atlantic Oscillation (NAO), *Geophys. Res. Lett.*, *30*(22), 2170, doi:10.1029/2003GL018545.

Palamara, D. R., and E. A. Bryant (2004), Geomagnetic activity forcing of the Northern Annular Mode via the stratosphere, *Ann. Geophys.*, *22*, 725–731.

Palmroth, M., T. I. Pulkkinen, P. Janhunen, D. J. McComas, C. W. Smith, and H. E. J. Koskinen (2004), Role of solar wind dynamic pressure in driving ionospheric Joule heating, *J. Geophys. Res.*, *109*, A11302, doi:10.1029/2004JA010529.

Palmroth, M., N. Partamies, J. Polvi, T. I. Pulkkinen, D. J. McComas, R. J. Barnes, P. Stauning, C. W. Smith, H. J. Singer, and R. Vainio (2007), Solar-wind magnetosphere coupling efficiency for solar wind pressure impulses, *Geophys. Res. Lett.*, *34*, L11101, doi:10.1029/2006GL029059.

Randall, C. E., et al. (2005), Stratospheric effects of energetic particle precipitation in 2003–2004, *Geophys. Res. Lett.*, *32*, L05802, doi:10.1029/2004GL022003.

Ruzmaikin, A., and J. Feynman (2002), Solar influence on a major mode of atmospheric variability, *J. Geophys. Res.*, *107*(D14), 4209, doi:10.1029/2001JD001239.

Salby, M. L., and P. F. Callaghan (2006), Relationship of the quasi-biennial oscillation to the stratospheric signature of the solar cycle, *J. Geophys. Res.*, *111*, D06110, doi:10.1029/2005JD006012.

Seppälä, A., P. T. Verronen, M. A. Clilverd, C. E. Randall, J. Tamminen, V. Sofieva, L. Backman, and E. Kyrölä (2007), Arctic and Antarctic polar winter NO_x and energetic particle precipitation in 2002–2006, *Geophys. Res. Lett.*, *34*, L12810, doi:10.1029/2007GL029733.

Shindell, D., D. Rind, N. Balachandran, J. Lean, and P. Lonergan (1999), Solar cycle variability, ozone, and climate, *Science*, *284*, 305–308.

Shue, J.-H., and Y. Kamide (2001), Effects of solar wind density on auroral electrojets, *Geophys. Res. Lett.*, *28*, 2181–2184.

Simmons, A. J., and J. K. Gibson (2000), The ERA-40 Project Plan, ERA-40 Project Report Series No. 1, 61 pp. (Available at: http://www.ecmwf.int/publications/library/ecpublications/_pdf/ERA40_PRS_1.pdf)

Siskind, D. E., G. E. Nedoluha, C. E. Randall, M. Fromm, and J. M. Russell (2000), An assessment of Southern Hemisphere stratospheric NO_x enhancements due to transport from the upper atmosphere, *Geophys. Res. Lett.*, *27*, 329–332.

Solomon, S., P. J. Crutzen, and R. G. Roble (1982), Photochemical coupling between the thermosphere and the lower atmosphere: 1. Odd nitrogen from 50 to 120 km, *J. Geophys. Res.*, *87*, 7206–7220.

Song, Y., and W. A. Robinson (2004), Dynamical mechanisms for stratospheric influences on the troposphere, *J. Atmos. Sci.*, *61*, 1711–1725.

Thejll, P., B. Christiansen, and H. Gleisner (2003), On correlations between the North Atlantic Oscillation, geopotential heights, and geomagnetic activity, *Geophys. Res. Lett.*, *30*(6), 1347, doi:10.1029/2002GL016598.

Thompson, D. W. J., and J. M. Wallace (1998), The arctic oscillation signature in the wintertime geopotential height and temperature fields, *Geophys. Res. Lett.*, *25*, 1297–1300.

Thompson, D. W. J., and J. M. Wallace (2000), Annular modes in the extratropical circulation. part I: Month-to-month variability, *J. Clim.*, *13*, 1000–1016.

Thompson, D. W. J., S. Lee, and M. P. Baldwin (2003), Atmospheric processes governing the Northern Hemisphere annular mode/North Atlantic Oscillation, in *The North Atlantic Oscillation*, *Geophys. Monogr.*, pp. 81–112, AGU.

van Loon, H., and J. C. Rogers (1978), The seesaw in winter temperature between Greenland and northern Europe, part 1: General description, *Mon. Weather Rev.*, *109*, 296–310.

Wang, Y. L., R. C. Elphic, B. Lavraud, M. G. G. T. Taylor, J. Birn, C. T. Russell, J. Raeder, H. Kawano, and X. X. Zhang (2006), Dependence of flux transfer events on solar wind conditions from 3 years of cluster observations, *J. Geophys. Res.*, *111*, A04224, doi:10.1029/2005JA011342.

Zhou, X. Y., and B. T. Tsurutani (1999), Rapid intensification and propagation of the dayside aurora: Large scale interplanetary pressure pulses (fast shocks), *Geophys. Res. Lett.*, *26*, 1097–1100.

Zhou, X. Y., and B. T. Tsurutani (2003), Dawn and dusk auroras caused by gradual, intense solar wind ram pressure events, *J. Atmos. Sol. Terr. Phys.*, *66*, 153–160.

———————

R. E. Hibbins, M. J. Jarvis, and H. Lu, Physical Sciences Division, British Antarctic Survey, High Cross, Madingley Road, Cambridge CB3 0ET, UK. (rehi@bas.ac.uk; mjja@bas.ac.uk; hlu@bas.ac.uk)